Title
Simulation and fabrication of 0–3 composite PZT films for ultrahigh frequency (100–300 MHz) ultrasonic transducers

Journal
Journal of Applied Physics, 119(9)

ISSN
0021-8979

Authors
Chen, Xiaoyang
Fei, Chunlong
Chen, Zeyu
et al.

Publication Date
2016-03-07

DOI
10.1063/1.4942857

Simulation and fabrication of 0–3 composite PZT films for ultrahigh frequency (100–300 MHz) ultrasonic transducers

Xiaoyang Chen,[1,2] Chunlong Fei,[3] Zeyu Chen,[3] Ruimin Chen,[3] Ping Yu,[2] Zhongping Chen,[1] K. Kirk Shung,[3] and Qifa Zhou[3]
[1]*Beckman Laser Institute & Medical Clinic and Department of Biomedical Engineering, University of California - Irvine, Irvine, California 92612, USA*
[2]*College of Material Science and Engineering, Sichuan University, Chengdu 610064, People's Republic of China*
[3]*Department of Biomedical Engineering and NIH Transducer Resource Center, University of Southern California, Los Angeles, California 90089, USA*

(Received 16 December 2015; accepted 14 February 2016; published online 1 March 2016)

This paper presents simulation, fabrication, and characterization of single-element ultrahigh frequency (100–300-MHz) needle ultrasonic transducers based on 0–3 composite $Pb(Zr_{0.52}Ti_{0.48})O_3$ (PZT) films prepared by using composite ceramic sol-gel film and sol-infiltration technique. The center frequency of the developed transducer at 300-MHz was the highest frequency of $PbTiO_3$ ceramic-based ultrasonic transducers ever reported. Furthermore, a brief description of the composite model was followed by the development of a new expression for predicting the longitudinal velocity, the clamped dielectric constant, and the complex electromechanical coupling coefficient k_t of these films, which is very important in ultrasonic transducer design. Moreover, these parameters are difficult to obtain by measuring the frequency dependence of impedance and phase angle because of the weak signal of the previous 0–3 composite films transducer (>100 MHz). The modeling results show that the Cubes model with a geometric factor $n = 0.05$ fits well with the measured data. This model will be helpful for developing the 0–3 composite systems for ultrahigh frequency ultrasonic transducer design. © *2016 AIP Publishing LLC*.
[http://dx.doi.org/10.1063/1.4942857]

I. INTRODUCTION

Recently, the ultra high frequency (UHF) ultrasonic transducer (>100-MHz) has attracted growing interests because its beam width could approach cellular dimension (micron size).[1] Moreover, the UHF transducers can be also applied to manipulate biological cells and micro-particles.[2,3] For the UHF transducer, its beam width is inversely proportional to the center frequency of transducer.[4] That suggests that the key to trap smaller size particle or cell is to develop the UHF ultrasonic transducers with higher center frequency. However, it is challenging and time consuming to build such UHF transducers using traditional approach in which piezoelectric ceramics or crystals are lapped down to the order of microns.[4] Piezoelectric thick film technology provides an alternative solution of controlling the film thickness within the accuracy of a few microns.[5,6] Among various thick film fabrication methods, the composite sol-gel film technique has been utilized successfully to fabricate the high frequency ultrasound transducers based on different types of piezoelectric thick films, including lead magnesium niobium/lead titanate (PMN/PT), potassium sodium niobate/bismuth sodium titanate (KNN/BNT), and PZT composite films.[6–8] The composite sol-gel technique is a modified sol-gel method by mixing ceramic powder with sol-gel solution and followed by optimized pyrolysis and annealing steps.[9,10] This approach has been utilized to fabricate dense and crack-free piezoelectric films in the range of 1–50-μm. Furthermore, the composite ceramic sol-gel film technique saves time and costs and is relatively easy to implement. However, the center frequency of the previously built UHF transducers using $PbTiO_3$ based composite films hardly exceeds 200-MHz due to the requirements of low porosity and high content of powder for the films.[6,7]

Currently, the Krimholtz, Leedom, and Matthaei (KLM) model has been used extensively in designing ultrasonic transducers.[10] Since the complex detailed material constants, including longitudinal velocity, density, clamped dielectric constant, coupling coefficient k_t, electrical loss tangent, and mechanical loss tangent, are given, the aperture size, shape, and materials thickness can be designed for any specific high frequency ultrasonic transducer applications. However, some parameters, including longitudinal velocity, clamped dielectric constant, and coupling coefficient k_t, are difficult to measure from the frequency dependence of impedance and phase angle when the film thickness is less than 10-μm because of the weak signal generated by the 0–3 composite film transducers (>100-MHz) previously built. Using other forms of measurements is both time and cost consuming. Thus, it is desirable to develop composite models for predicting the mechanical, electrical, and electromechanical properties.[11–14] This simulation process is not easy due to complexity of a two-phase system (sol and powder), in which many permutations and combinations are possible,[15] including powder to sol ratio, size of powder, quality, and composition of powder.[16] In addition, the sol-infiltration technique used in our experiments complicates the simulation process further by introducing more sol. Spring models, such as Voigt, Reuss, and Cubes model, assuming that the structure of 0–3

composite systems is composed by springs with different combinations, have been used to predict the longitudinal velocity.[16,17] However, there is much less work reported on the calculation of k_t in 0–3 composite systems.

In our study, the sol-infiltration process was used to improve film quality and maintain low porosity of films.[18–21] Through this method, the PZT composite films transducer operating at frequencies higher than 300-MHz was obtained, which is the highest center frequency of $PbTiO_3$ based composite films ultrasonic transducers ever reported for their higher dielectric loss compared with other ferroelectric materials. In addition, the longitudinal velocity was calculated by taking into account the sol-infiltration process. Furthermore, we calculated the k_t of 0–3 composite films from the view of energy conversion and the spring model. Then, 80-MHz 0–3 composite films ultrasonic transducer with the same powder to sol ratio and process was used to measure the coupling coefficient k_t in thickness mode to verify the calculation. The modelling clamped dielectric constant was obtained from the spring model and the calculated k_t. Finally, the center frequency and the electrical input impedance between the measured and calculated results were compared to evaluate the accuracy of the simulation.

II. EXPERIMENTAL METHODS

A. PZT composite film

In this work, a sol-gel composite method was used to prepare PZT composite films. A 2-methoxyethanol-based sol-gel $Pb(Zr_{0.52}Ti_{0.48})O_3$ (PZT) precursor was used as the matrix. A PZT 5H powders (Piezoelectric Technology Inc.) were used as the loading powder in the composite sol-gel. Then, these powders were ball milled for 32 h at 200 rpm in ethanol using a Fritsch Pulverisette milling machine (Fritsch GmbH, Idar-Oberstein, Germany). After ball milling, the average particle size of powder is about 250-nm. Afterwards, these powders were mixed with PZT sol-gel precursor with the powder to solution mass ratios of 1:4. The solution to powder mass ratios of 4 would lead to the volume fraction of powder with a value of 65% through the calculation from the density of powder, and the powder crystallized from the sol-gel, density, and concentration of the precursor and the solution to powder mass ratio. Then, the composite solutions were ball milled for 20 h to obtain well-dispersed composite solution. Finally, the prepared composite solutions were spin-coated onto $Pt/Ti/SiO_2/Si$ substrates, at a speed of 2000 rpm for 30 s. A two-step pyrolysis scheme was conducted on each deposited layer with a first pyrolysis step at 200 °C for 2 min and then followed by a second step at 400 °C for 2 min in air. Subsequently, each PZT layer was annealed by a rapid thermal annealing (RTA) process at 750 °C for 1 min. To minimize or reduce the porosity for higher dense thick PZT films, a vacuum infiltration of the PZT sol-gel solution process was taken into the as prepared PZT composite layer. First, pure PZT precursor solution was evenly dispersed onto the film surface after each composite PZT layer was deposited. Subsequently, the film was put into a vacuum (~30 psi) for 30 s to improve the solution penetration into the pores and followed by the spinning and pyrolysis procedures as mentioned above.[12]

The composite films with desired thickness were obtained by repeating the spinning–heating-infiltrating-spinning-heating process. Finally, the deposited films were annealed by a conventional thermal annealing (CTA) at 750 °C for 3 h in air. In our experiments, the samples with thickness of 3.5 μm, 3.7 μm, 6.4 μm, and 10 μm were fabricated by this method, and the number of sol-infiltration times was 9, 10, 15, and 20, respectively.

The spinning–heating-infiltrating-spinning-heating process is effective to make every layer dense, flat, and with reduction in porosity. The presence of significant levels of porosity could result in lower values of dielectric constant and makes films easily broken down in the poling process when applied by a high voltage. This porosity is very detrimental for developing thinner films for UHF application. Our approach can lower porosity to the minimum level and maintains high powder loading. However, by using this sol-infiltration technique, a much lower values of relative permittivity (~900) layer crystallized from pure PZT precursor solution were formed between every layer with the thickness of 100 nm, as shown in Fig. 1. This low dielectric layer should be included in the simulation for a more accurate prediction.

B. Fabrication and evaluation of transducer

The PZT composite film ultrasonic transducers were fabricated using conventional transducer fabrication technology.[6,7] The composite films with thicknesses ranging from 3.5 to 10 μm were used to fabricate the UHF transducers (>100 MHz). First, a very lossy conductive epoxy (E-Solder 3022, Von Roll Isola Inc., New Haven, CT) with an acoustic impedance of ~6 MRayl was cast to the film as the backing material by centrifuging it at 3000 rpm for 15 min. After curing overnight at room temperature, the backing layer was lapped down to 1-mm thick. Subsequently, the samples were diced along the thickness direction into small squares with dimensions of $0.4 \times 0.4\text{-mm}^2$ for 10-μm and 6.4-μm samples, and $0.2 \times 0.2\text{-mm}^2$ for 3.7-μm and 3.5-μm samples. The film with the support of the backing layer was removed from the Si substrate without any damage through the wet

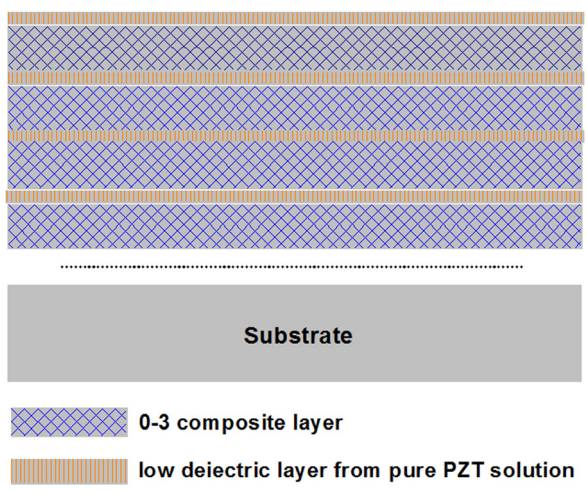

FIG. 1. Schematic diagram of 0–3 composite PZT films.

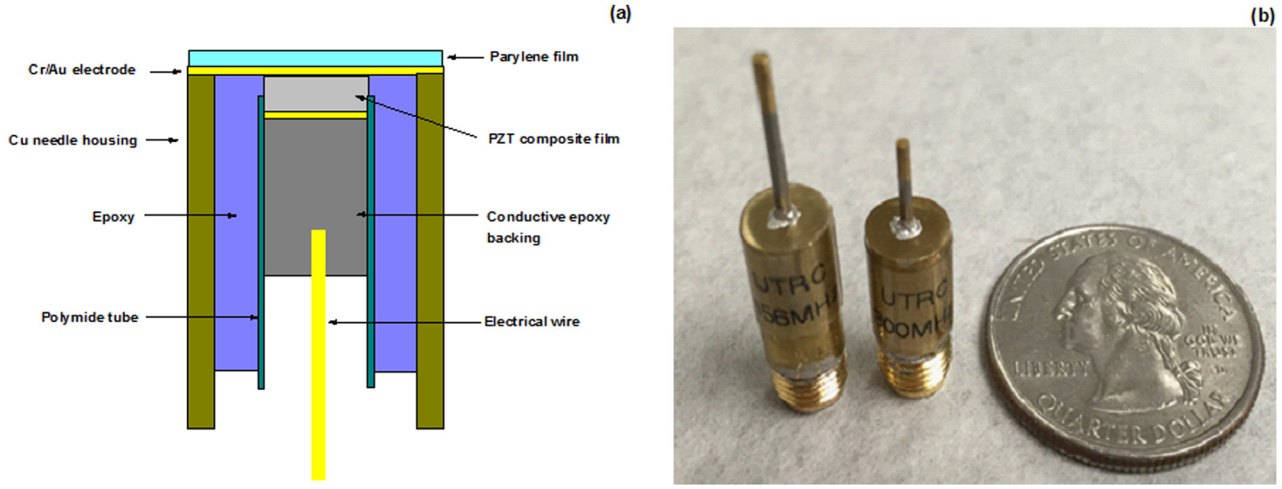

FIG. 2. A cross sectional view of (a) design and (b) photograph of the final transducer prototype.

etching process by soaking samples to KOH solution with the concentration of 20% at 80 °C for 5 to 10 min.[18] Then, the acoustic stack was inserted into a polyimide tube (Small Parts Inc., Miramar, FL), which served as an insulating layer. A lead wire was connected to the backing layer by injecting conductive epoxy to polyimide tube. The piezoelectric element was fixed into a steel needle housing and followed by filling the gap between the element and housing using epoxy (Epotek-301, Epoxy Technology Inc., Billerica, MA). A Cr/Au (500 Å/1000 Å) layer was sputtered across the piezoelectric element and the needle housing to serve as a ground. A 1-μm thick parylene layer was vapor-deposited on front face of the transducer to serve as an acoustic matching layer and a protection layer. The final transducer was assembled with an SMA connector for further poling and pulse-echo measurement. The transducer was poled with an electric field of 150 kV/cm (about three times of the coercive field) for 5-min at 120 °C. A cross sectional view of the design and photograph of the final transducer prototype is shown in Fig. 2.

Performance of the transducer was evaluated in deionized water using conventional pulse-echo response measurement. During the measurement, the transducer was connected to a pulser/receiver (JSR Ultrasonics DPR 500, Imaginant, Pittsford, NY) and excited by an electrical impulse at 200-Hz repetition rate, 50-Ω damping, and 2.3-μJ energy per pulse. An X-cut quartz plate was used as a target. The center frequency and the −6-dB bandwidth were determined from the measured frequency spectrum.

C. Review of composite model

The ultrasonic transducer emitted well-damped pulse in the measurements. This means that the ultrasonic measurement was conducted at high strain rates with very little displacement, so that only the elastic properties affected the measurements and plastic deformation was negligible.[16] Thus, using spring model to predict the elastic properties is valuable. For the application of ultrasonic transducer using 0–3 composite materials, elastic constant along the thickness direction is of interest. There are three different models to calculate longitudinal elastic modulus of composite materials as a function of volume fraction of the constituents. The Voigt model (parallel springs) assumes continuous strain in the two constituents. The Reuss model (series springs) assumes continuous stress in the two constituents. The Cubes model assumes a combination of series and parallel springs in the two constituents.[11,16] In order to improve the versatility of this model, Banno introduced a geometric factor "n" into Cubes model. Varying the geometric factor "n" allows the Cubes model to vary between the series and parallel springs' models. The value of "n" is depending on an attempt to match calculation with experimental observation. These three models are illustrated in Fig. 3 and indicated below.

Voigt model (parallel springs)[11,16]

$$E = V_1E_1 + (1 - V_1)E_2. \tag{1}$$

Reuss model (series springs)[11,16]

$$\frac{1}{E} = \frac{V_1}{E_1} + \frac{1 - V_1}{E_2}. \tag{2}$$

Cubes model (parallel springs and series springs together)[11,22]

$$E = \frac{a^2(a + (1 - a)n)^2E_1E_2}{aE_2 + (1 - a)nE_1} + E_2\left(1 - a^2(a + (1 - a)n\right)\left(V_1 = a^3\right), \tag{3}$$

where E = longitudinal elastic modulus of composite, E_1 = longitudinal elastic modulus of powder, E_2 = longitudinal elastic modulus of PZT matrix crystallized from pure PZT sol-gel precursor, V_1 = volume fraction of powder, and the geometric factor $n = 0.05$ and 1.0 in our article.

III. RESULTS AND DISCUSSION

A. Simulation

1. Longitudinal velocity

For the single-element transducer, its thickness t determines the resonance frequency of the transducer by the equation below[23]

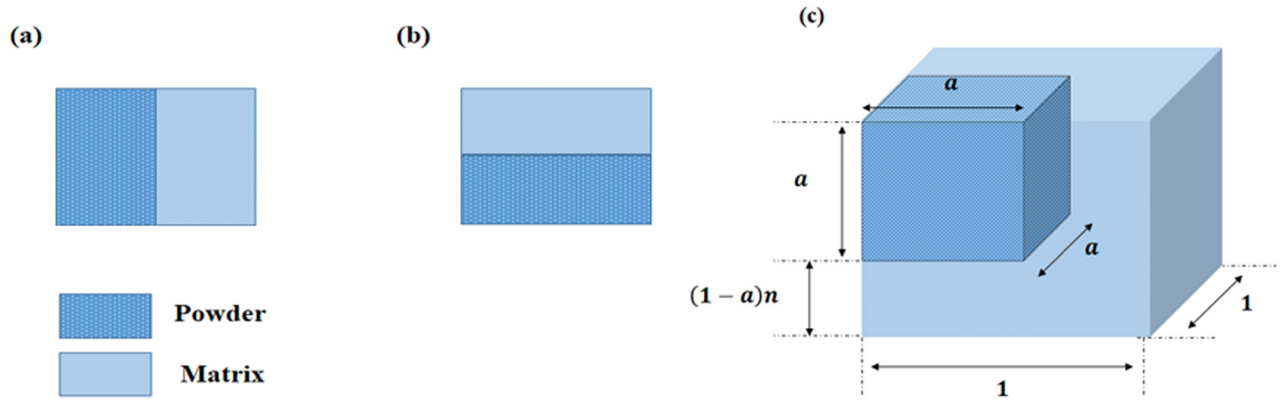

FIG. 3. Geometry of springs' models: (a) Vogit model, (b) Reuss model, and (c) modified Cubes model.

$$t=\frac{C_L}{2f_t}, \tag{4}$$

where f_t is the resonance frequency of the longitudinal thickness vibration, C_L is the longitudinal velocity of sound, and t is the thickness of films. The center frequency obtained from the pulse echo measurement can be used to estimate the longitudinal velocity of sound of films. Simply, the longitudinal velocity is related to the elastic properties of the materials by the equation below

$$C_L = \sqrt{c_{33}^D/\rho} = \sqrt{E/\rho}, \tag{5}$$

where c_{33}^D is the open circuit complex elastic stiffness, E and ρ are the longitudinal elastic modulus and the density of materials, respectively.

Fig. 4(a) shows the longitudinal velocity of sound in 0–3 composite films as a function of powder volume fraction, obtained from the Voigt, Reuss and Cubes model.

In this study, except for the calculation of 0–3 composite systems, the low value of dielectric constant layer mentioned before should be considered as a spring connecting adjacent layers in series

$$\frac{nd_i}{E_i}+\frac{d_{0-3}}{E_{0-3}}=\frac{nd_i+d_{0-3}}{E}, \tag{6}$$

where E_i = longitudinal elastic modulus of low dielectric layer, E_{0-3} = longitudinal elastic modulus of 0–3 composite layers, n = sol-infiltration times, d_i = the thickness of low dielectric layer (~100 nm), and d_{0-3} = the thickness of 0–3 composite layers.

Fig. 4(b) shows the dependence of film thickness on the longitudinal velocity of sound including the low dielectric layers. By taking into account the sol-infiltration process, the longitudinal velocity of sound of 0–3 composite films was thickness dependent.

2. Electromechanical coupling coefficient k_t

It was mentioned before that it was difficult to obtain k_t from the frequency dependence of impendence and phase angle, since the film thickness is less than 10 μm and produces weak signal for previously fabricated 0–3 composite film transducers (>100 MHz). However, the spring model can be used to estimate the complex electromechanical coupling coefficient k_t from the perspective of energy conversion. For the ultrasonic transducer application, the piezoelectric effect can be expressed as the constitutive equations

$$X = c^D x - \mathrm{hD}, \tag{7}$$

$$\mathrm{E} = -h + \kappa^x \kappa_0 D, \tag{8}$$

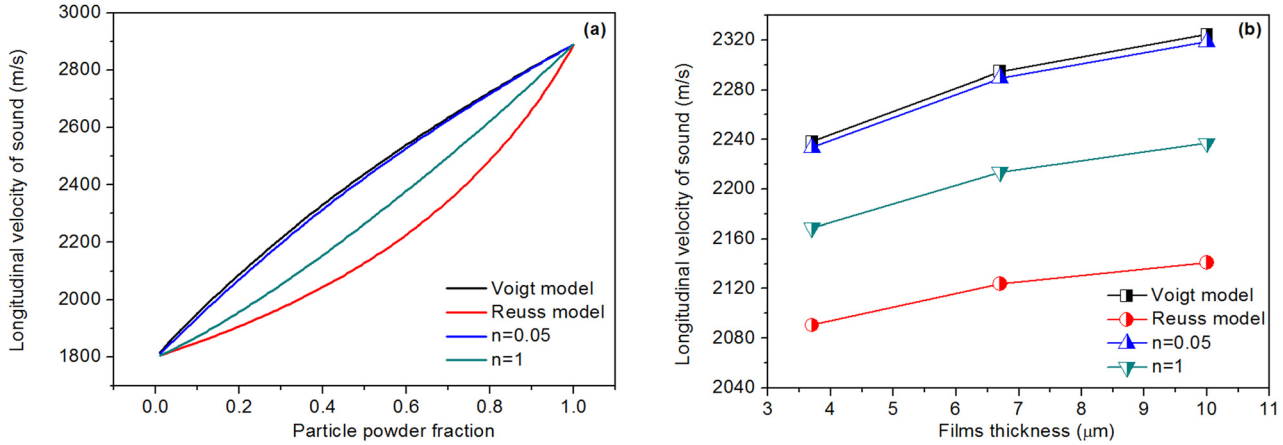

FIG. 4. Comparison of the calculated longitudinal velocity of sound of 0–3 composite films with various particle volume fractions and film thicknesses obtained from the Voigt, Reuss, and Cubes model: (a) dependence of powder volume fraction on the longitudinal velocity of sound and (b) dependence of film thickness on the longitudinal velocity of sound while considering the low dielectric layers.

where x is the strain, X is the stress, D is the electric displacement, E is the electric field, c^D the is open circuit complex elastic stiffness, $\kappa^x = 1/\varepsilon^x$ is the clamped dielectric constant, and h is the piezoelectric constant.

For the mechanical energy into electrical energy of the ultrasonic transducer:

The input mechanical energy, the stored mechanical and elastic energies can be calculated as[24]

$$\text{Total input mechanical energy}: U_m = \frac{1}{2}c^D x^2. \tag{9}$$

Stored mechanical energy (electrically short–circuited):

$$\frac{1}{2}c^E x^2.$$

Stored electrical energy (mechanically clamped) :

$$U_{\text{me}} = \frac{1}{2}\frac{h^2 x^2}{\kappa_0 \kappa^x}. \tag{10}$$

The complex electromechanical coupling :

$$k_t^2 = \frac{U_{\text{me}}}{U_m} = h_{33}^2 \varepsilon_{33}^x / c_{33}^D. \tag{11}$$

Assuming the complex coupling effect between the powder and the matrix was not taken into account, the k_t of 0–3 composite film systems can be presented as

$$k_t = \left(\frac{U_{\text{me1}} + U_{\text{me2}}}{U_m}\right)^{1/2} = \left(\frac{U_{m1}k_{t1}^2 + U_{m2}k_{t2}^2}{U_m}\right)^{1/2}, \tag{12}$$

where U_m, U_{m1}, and U_{m2} are the total input mechanical energy of composite material, powder, and matrix, respectively. U_{me1} and U_{me2} are the stored electrical energy of the powder and matrix, respectively. k_{t1} and k_{t2} are the k_t of powder and matrix.

Based on the spring connectivity, the Voigt, Reuss, and modified Cubes model would be used to calculate the k_t of 0–3 composite film systems.

Voigt model (parallel springs)

$$k_t = \left(\frac{V_1 k_{t1}^2 c_1^D + (1-V_1)c_2^D k_{t2}^2}{1/c^D}\right)^{1/2} = \left(V_1 k_{t1}^2 E_1 + \left(\frac{(1-V_1)E_2 k_{t2}^2}{1/E}\right)^{1/2}\right)^{1/2}. \tag{13}$$

Reuss model (series springs)

$$k_t = \left(\frac{V_1 k_{t1}^2 c_1^D + (1-V_1)c_2^D k_{t2}^2}{c^D}\right)^{1/2} = \left(V_1 k_{t1}^2 E_1 + \left(\frac{(1-V_1)E_2 k_{t2}^2}{E}\right)^{1/2}\right)^{1/2}, \tag{14}$$

where k_t = the electromechanical coupling k_t of composite films, k_{t1} = the k_t of powder, k_{t2} = the k_t of PZT matrix, c_1^D = the open circuit complex elastic stiffness of PZT powder, and c_2^D = the open circuit complex elastic stiffness of PZT matrix.

Here, we use the modified Cubes model to calculate the k_t

$$\text{For the matrix part}: \left(1 - a^2(a + (1-a)n)\right)E_2 k_{t2}^2 + k_{t2}^2\left(\frac{a^2(a+(1-a)n)^2 E_1 E_2}{aE_2 + (1-a)nE_1}\right)^2 \Big/ E_2.$$

$$\text{For the powder part}: k_{t1}^2\left(\frac{a^2(a+(1-a)n)^2 E_1 E_2}{aE_2 + (1-a)nE_1}\right)^2 \Big/ E_1.$$

So there is equation for the k_t

$$k_t = \left(\frac{(1 - a^2(a+(1-a)n))E_2 k_{t2}^2 + k_{t2}^2\left(\frac{a^2(a+(1-a)n)^2 E_1 E_2}{aE_2 + (1-a)nE_1}\right)^2 \Big/ E_2 + k_{t1}^2\left(\frac{a^2(a+(1-a)n)^2 E_1 E_2}{aE_2 + (1-a)nE_1}\right)^2 \Big/ E_1}{E}\right)^{1/2}. \tag{15}$$

Generally, the sol-gel synthesized PZT matrix has poorer performance. As a result, it is hypothesized that to simplify the calculation, the sol-gel synthesized PZT matrix does not contribute to k_t.

Under this condition, the equation can be expressed as

$$k_t = k_{t1}\frac{a^2(a+(1-a)n)^2 E_1 E_2}{aE_2 + (1-a)nE_1}\frac{1}{\sqrt{E_1 E}}. \tag{16}$$

Similarly, the low value of the dielectric constant layer mentioned before should be considered as a spring connecting adjacent layers in series to calculate k_t by using Equation (14). Finally, the calculated results of k_t of 0–3 composite films with various powder volume fractions and film thicknesses obtained from the Voigt, Reuss, and Cubes model are presented in Fig. 5. It was found that the influence of geometric factor n on the value of k_t is much smaller than the longitudinal speed of sound.

In order to check the correctness of the calculated value of k_t, the 0–3 composite films ultrasonic transducer at a center frequency of 80 MHz is fabricated to measure k_t with the same fabrication process and powder volume fraction, as shown in Fig. 6. Simultaneously, the calculated values of k_t obtained from the Voigt, Reuss, and Cubes model are 0.379, 0.162, 0.322 ($n = 0.05$), and 0.305 ($n = 1$), respectively. The measured 80 MHz transducer shows a value of k_t of 0.32, which is very close to the modified Cubes model when $n = 0.05$. This indicates that the Cubes model can be used to estimate k_t of 0–3 composite films.

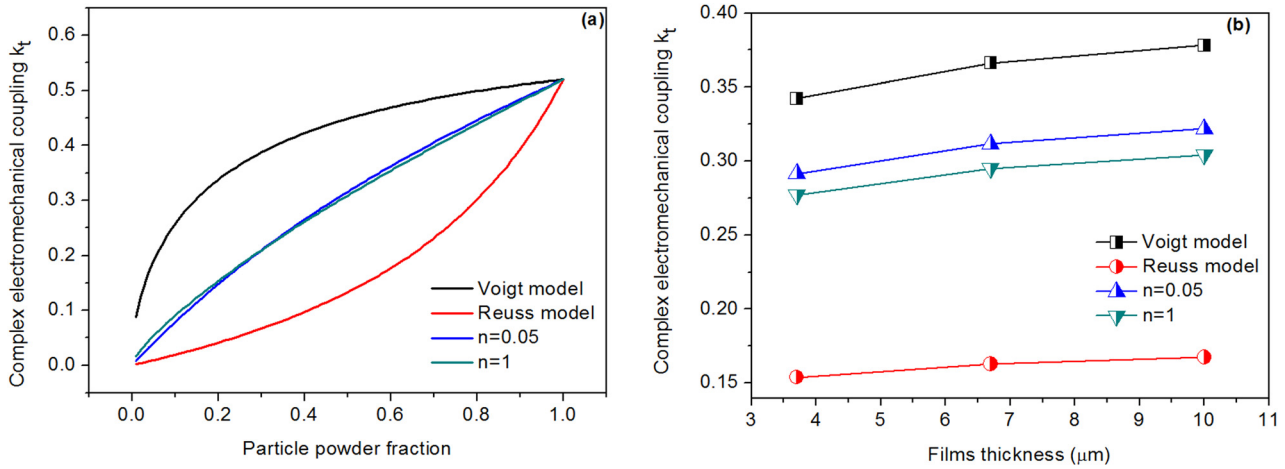

FIG. 5. Comparison of k_t of 0–3 composite films with various particle fractions and thicknesses obtained from the Voigt, Reuss, and Cubes model: (a) dependence of particle powder fraction on the k_t and (b) dependence of film thickness on the longitudinal velocity of sound including the low dielectric layers into consideration.

3. The clamped dielectric constant ε_{33}^{s}

The calculation of k_t is also important for calculating the clamped dielectric constant of 0–3 composite films. The frequency dependence of impedance and phase angle cannot be measured when the film thickness is less than 10 μ m, which also means that the clamped dielectric constant is difficult to measure as well. However, the relationship between the k_t and the dielectric constant can be used to calculate the clamped dielectric constant.[25]

For a circular disc model, it is known that

$$\varepsilon_{33}^{S} = \left(1 - k_t^2\right)\left(1 - k_p^2\right)\varepsilon_{33}^{T} = \left(1 - k_t^2\right)\varepsilon_{33}^{P}, \qquad (17)$$

where ε_{33}^{s}, ε_{33}^{T}, and ε_{33}^{P} are the overall clamped dielectric constant, the free clamped dielectric constant, and the partly clamped dielectric constant, respectively. The symbols k_t and k_p are the complex electromechanical coupling of thickness extension vibration and radial vibration model. For the single element transducer, the element is surrounded by epoxy, as shown in Fig. 2. It may be assumed that the element is clamped by epoxy along the radial vibration direction (the epoxy is very rigidity). In this situation, the dielectric constant of 0–3 composite film transducers measured at 1 kHz is close to the ε_{33}^{P}. Fig. 7 shows the comparison between the dielectric constant of ultrasonic transducer and the clamped dielectric constant calculated from the spring model by using the calculated k_t before.

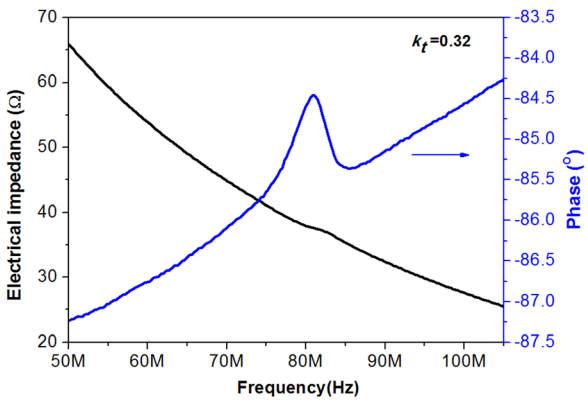

FIG. 6. The frequency dependence of impedance and phase angle of a 80 MHz ultrasonic transducer fabricated by using 0–3 composite PZT films with the same volume powder volume fraction.

B. Dielectric and ferroelectric properties measurements

The XRD pattern of PZT composite films on a Pt/Si wafer is shown in Fig. 8(a). It shows that the pure perovskite phase of PZT ceramic films was synthesized successfully without any pyrochlore phase presented in the XRD patterns. The well crystallized perovskite phase indicated a high-quality film. The ferroelectric hysteresis loops of 0–3 composite films of different thicknesses are shown in Fig. 8(b). It was found that the coercive field *Ec* increased with decreasing thickness, while all samples kept approximate value of maximum polarization and remnant polarization. Depending on the fabrication of 0–3 composite films, this pinning of domain wall motion does not appear to come from porosity. It is related to the formation of layers of low relative permittivity between adjacent layers in the sol-infiltration process.

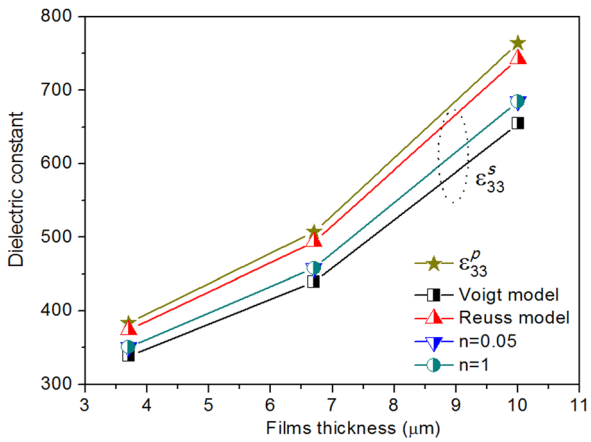

FIG. 7. The dielectric constant of 0–3 composite films ultrasonic transducer measured at 1 kHz and the clamped dielectric constant calculated by using different spring models.

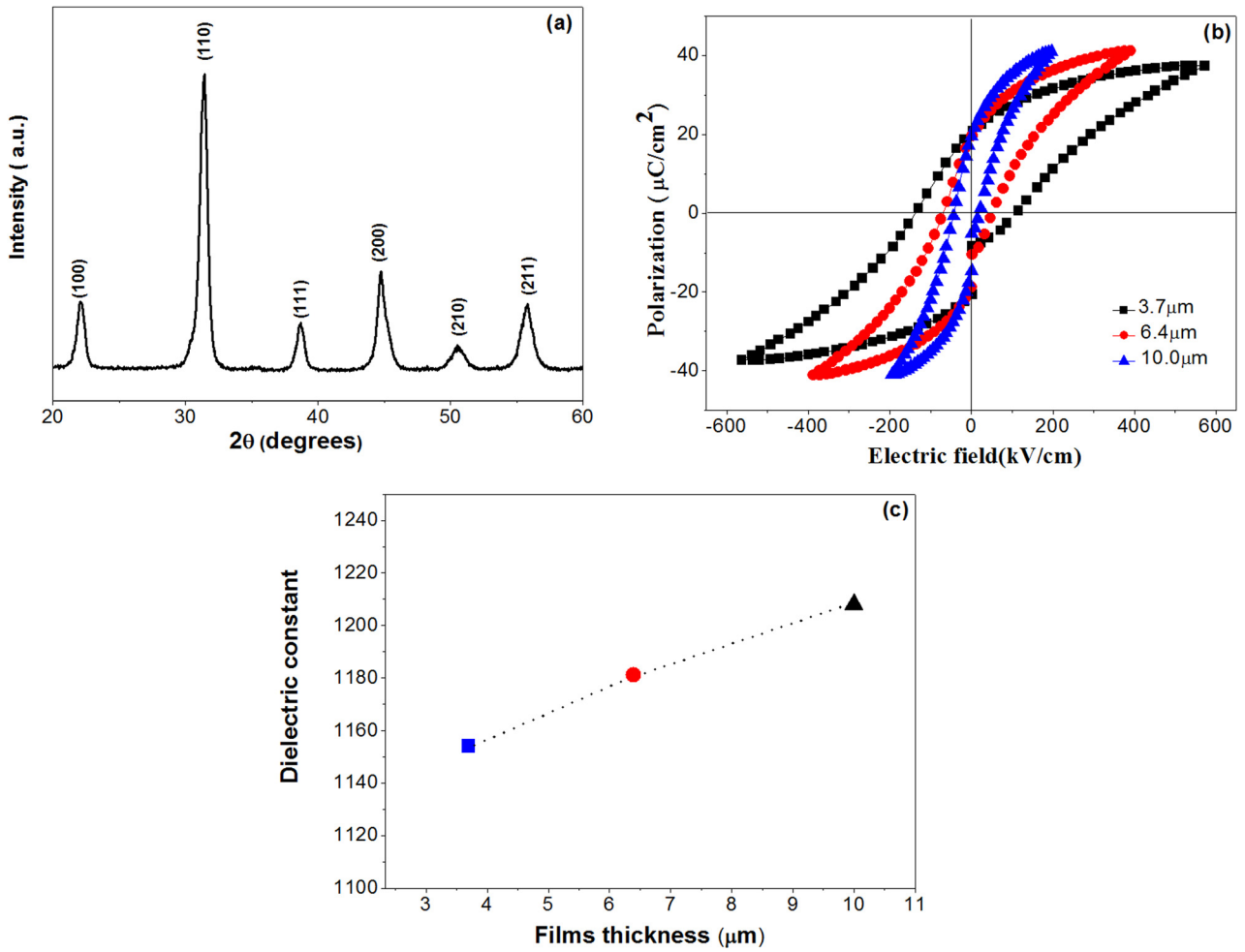

FIG. 8. XRD patterns of 0–3 composite films with a thickness of 10 μm (a), polarization-electric field hysteresis loops (b) and the measured dielectric constant (c) of 0–3 composite films with the different thicknesses on the Pt substrate.

Fig. 8(c) shows the measured dielectric constant of 0–3 composite films with various thicknesses. It is interesting to find that the dielectric property of these 0–3 composite films is thickness dependent, perhaps caused by the fabrication process. It was noticed that the film thickness was not proportional to infiltrating times, which is caused by the uneven distribution of the powder in the sol-gel precursor solution and increasing film surface roughness. Each time one performs the spinning coating process will lead to deviation.

C. Ultrasonic measurements

The composite film transducers were fabricated at ultrahigh center frequencies in the 100–300 MHz range. The receive-echo response and frequency spectra of the transducers are shown in Fig. 9. In this study, the highest center frequency of the transducer was 301 MHz as shown in Fig. 9(d), which is the highest value of the PZT based ceramic ultrasonic transducer ever reported. Compared to the previous devices, the transducer performance has been improved. By using thinner composite films, the center frequency range of the transducers has been increased. However, the bandwidth became narrower and echo signal weaker with an increase of frequency. This is expected given the increased attenuation of sound in water as frequency increases. Moreover, for the development of a higher frequency ultrasonic transducer, a smaller aperture is desired for the electrical impedance match. In our experiments, the element size of 301 MHz ultrasonic transducer was only 0.2×0.2 mm. This may present as a big challenge for developing a smaller size element for the higher frequency transducer by dicing.

D. Evaluation of the calculation

Since the clamped dielectric constant, the complex coupling efficient, and the longitudinal velocity of sound of 0–3 composite films can be obtained from our model. These parameters can be entered into KLM model to validate these calculations. At the same time, attenuation of ultrasound in the load medium (water) is also taken into the calculation. We here focus only on the comparison of the center frequency and the electrical input impedance between the measured value and the calculated value, because the echo signal is affected by many more parameters including measurement condition (such as cable length and equipment setting).[1] As shown in Fig. 10, the modeled center frequency of ultrasonic transducer is very close to the measured value, especially at $n = 0.05$ for the Cubes model and Voigt model. The 3.7 μm samples have a higher impedance than the 6.7 μm ones, which is caused by the smaller aperture size mentioned in

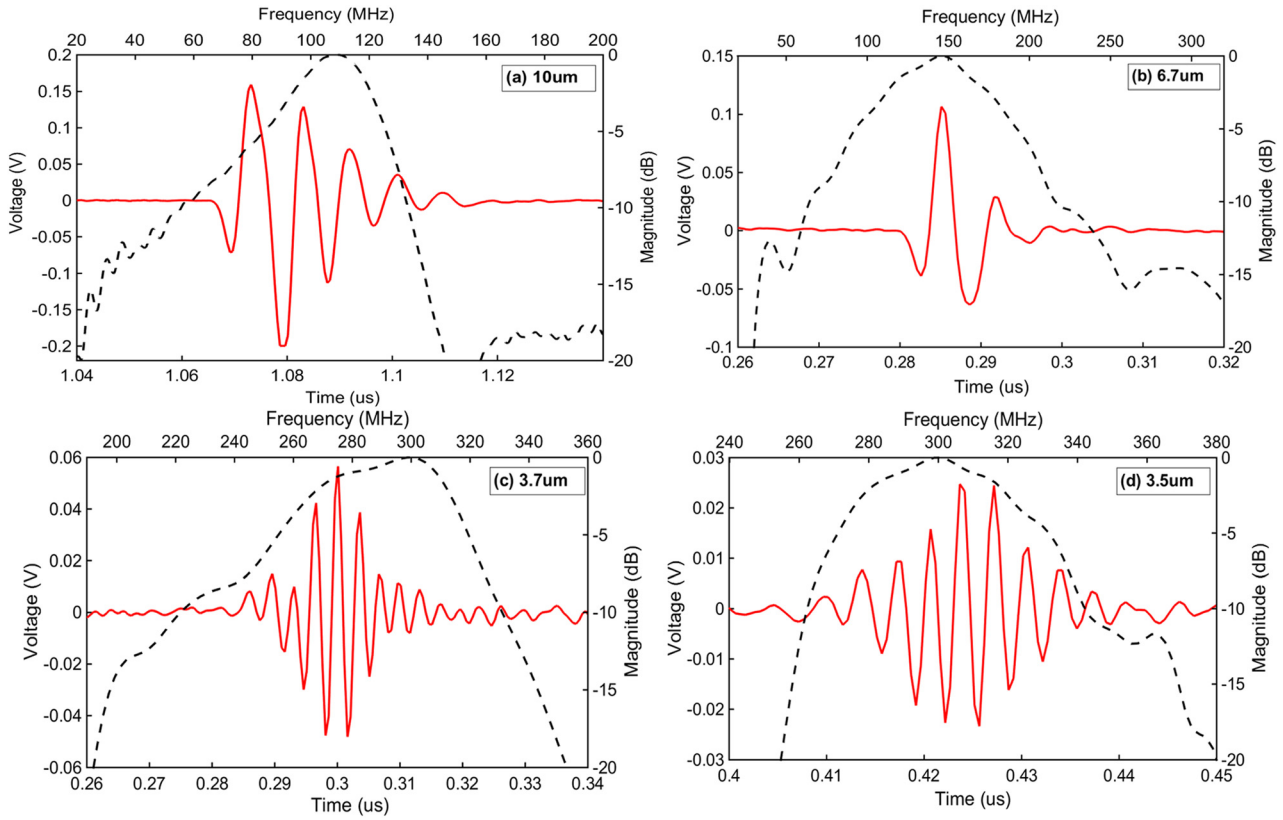

FIG. 9. Measured pulse-echo waveform (solid line) and normalized spectrum (dashed line) for PZT composite film transducer: (a) 103 MHz, (b) 156 MHz, (c) 286 MHz, and (d) 301 MHz.

the experimental part. Through the analysis above, the $n = 0.05$ Cubes model yields the best estimation of k_t of the real value. In the Conclusion, it is fair to say that the $n = 0.05$ Cubes model is capable of providing an accurate estimation of k_t, ε_{33}^s, and longitudinal velocity of sound in 0–3 composites.

IV. CONCLUSIONS

This paper presents the fabrication and characterization of single-element ultrahigh frequency (100–300-MHz) needle ultrasonic transducers based on 0–3 composite PZT films by combining the composite ceramic sol-gel film technique and sol-infiltration technique. The center frequency of 300-MHz is the highest value in a $PbTiO_3$ based ceramic ultrasonic transducers ever reported. These UHF transducers would be useful for developing biomedical applications, including very high scanning acoustic microscopy, cell stimulation, and particle manipulation. Combining with a detailed fabrication process, the spring model developed in this work appears to be a valid tool in the predicting the longitudinal velocity, the clamped dielectric constant, and the

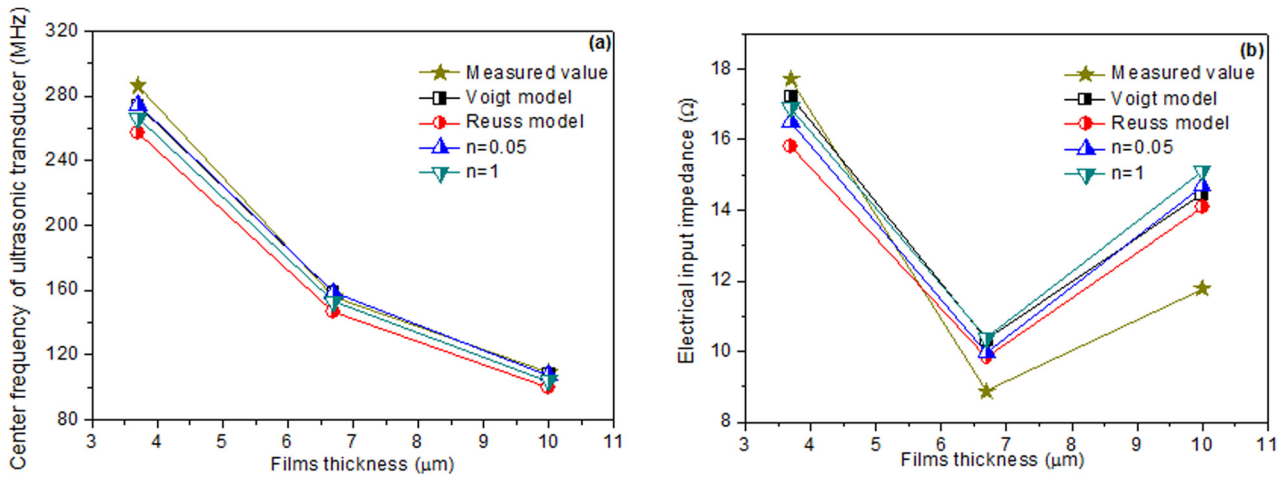

FIG. 10. Comparison of the measured and the calculated center frequency (a) and the electrical input impedance (b) of 0–3 composite films ultrasonic transducer with various thicknesses obtained from the Voigt, Reuss, and Cubes model through PiezoCAD.

complex electromechanical coupling coefficient k_t. This is important for the design of a specific UHF ultrasonic transducer application based on the 0–3 composite films using KLM model. The modeling results also show that the Cubes model with a geometric factor $n = 0.05$ best predicts these parameters.

ACKNOWLEDGMENTS

This work was supported by the National Institutes of Health (Grant No. P41-EB002182) and the China Scholarship Council (CSC).

[1]K. H. Lam, H. F. Ji, F. Zheng, W. Ren, Q. Zhou, and K. K. Shung, Ultrasonics **53**, 1033 (2013).
[2]J. Lee, S. Y. Teh, A. Lee, H. H. Kim, C. Lee, and K. K. Shung, Appl. Phys. Lett. **95**, 073701 (2009).
[3]J. Lee, K. Ha, and K. K. Shung, J. Acoust. Soc. Am. **117**, 3273 (2005).
[4]K. H. Lam, H. S. Hsu, Y. Li, C. Lee, A. Lin, Q. F. Zhou, and K. K. Shung, Biotechnol. Bioeng. **110**, 881 (2013).
[5]Q. F. Zhou, S. T. Lau, D. W. Wu, and K. Shung, Prog. Mater. Sci. **56**, 139 (2011).
[6]H. S. Hsu, V. Benjauthrit, F. Zheng, R. Chen, Y. Huang, Q. Zhou, and K. K. Shung, Sens. Actuators, A **179**, 121 (2012).
[7]B. P. Zhu, D. W. Wu, Q. F. Zhou, J. Shi, and K. K. Shung, Appl. Phys. Lett. **93**, 012905 (2008).
[8]S. T. Lau, H. F. Ji, X. Li, W. Ren, Q. Zhou, and K. K. Shung, IEEE Trans. Ultrason., Ferroelectr., Freq. Control **58**, 249 (2011).
[9]D. A. Barrow, T. E. Petroff, and M. B. A. Q. U. Sayer, Surf. Coat. Technol. **76**, 113 (1995).
[10]S. Sherrit, S. P. Leary, B. P. Dolgin, and Y. Bar-Cohen, in *Proceedings of the 1999 Ultrasonics Symposium* (1999), pp. 921–926.
[11]J. A. Hossack and B. A. Auld, in *Proceedings of the 1995 Ultrasonics Symposium* (1995), pp. 945–949.
[12]V. Y. Topolov and C. R. Bowen, *Electromechanical Properties in Composite Based on Ferroelectrics* (Springer Science & Business Media, London, 2009), p. 11.
[13]C. R. Bowen and V. Y. Topolov, Acta Mater. **51**, 4965 (2003).
[14]M. T. Sebastian and H. Jantunen, Int. J. Appl. Ceram. Technol. **7**, 415 (2010).
[15]A. Sachdeva and R. P. Tandon, Ceram. Int. **38**, 1331 (2012).
[16]S. Lees and C. L. Davidson, IEEE Trans. Sonics Ultrason. **SU-24**, 222 (1977).
[17]T. R. Gururaja, W. A. Schulze, L. E. Cross, R. E. Newnham, B. A. Auld, and Y. J. Wang, IEEE Trans. Sonics Ultrason. **32**, 481 (1985).
[18]D. L. Corker, Q. Zhang, R. W. Whatmore, and C. Perrin, J. Eur. Ceram. Soc. **22**, 383 (2002).
[19]D. Wu, Q. Zhou, K. K. Shung, S. N. Bharadwaja, D. Zhang, and H. Zheng, J. Am. Ceram. Soc. **92**, 1276 (2009).
[20]D. A. Barrow, T. E. Petroff, R. P. Tandon, and M. Sayer, J. Appl. Phys. **81**, 876 (1997).
[21]R. A. Dorey, S. B. Stringfellow, and R. W. Whatmore, J. Eur. Ceram. Soc. **22**, 2921 (2002).
[22]H. Banno and S. Saito, Jpn. J. Appl. Phys. **22**, 67 (1983).
[23]K. K. Shung, *Diagnostic Ultrasound: Imaging and Blood Flow Measurements* (CRC Press, Boca Raton, 2006), p. 39.
[24]K. Uchino, J. H. Zheng, and Y. H. Chen *et al.*, J. Mater. Sci. **41**, 217 (2006).
[25]A. V. Mezheritsky, IEEE Trans. Ultrason., Ferroelectr., Freq., Control **50**, 1742 (2003).